Current Topics in Biochemical Research
Vol. 14, *1*, 2012

Original Communication

Mass spectrometry-based proteomic assessment of the *in vitro* toxicity of carbon nanotubes

P. Kumarathasan[1,*,#], D. Das[1,#], M. A. Salam[1], S. Mohottalage[1], N. DeSilva[2], B. Simard[3], and R. Vincent[4]

[1]Analytical Biochemistry and Proteomics Laboratory, Mechanistic Studies Division, Environmental Health Sciences and Research Bureau, Healthy Environments and Consumer Safety Branch, Health Canada, Ottawa, Ontario, K1A 0K9, [2]Department of Earth Science, University of Ottawa, Ottawa, Ontario, K1N 6N5, [3]NRC Steacie Institute for Molecular Sciences, Ottawa, Ontario, K1A 0R6, [4]Inhalation Toxicology Laboratory, Hazard Identification Division, Environmental Health Sciences and Research Bureau, Healthy Environments and Consumer Safety Branch, Health Canada, Ottawa, Ontario, K1A 0K9, Canada

ABSTRACT

Due to the unique size-specific properties, carbon nanotubes (CNTs) have been incorporated in several industrial processes and consumer products, thereby increasing the likelihood of some human exposure. However, the few studies on toxicity of CNTs in the literature are often not comparable, due in part to lack of information on physicochemical characteristics. We have compared the biological responses of J774 murine macrophages exposed to four well characterized nanomaterials: single-walled and multi-walled, pristine and oxidatively-modified CNTs, at a dose range of 0-100 μg/cm^2. Viability was assessed by AlamarBlue and MTS reduction. Cell supernatants were analyzed for oxidatively modified protein metabolites by HPLC-coulometric array detection. Shot-gun proteomic analyses of direct and tryptic-digested cell lysates were performed by MALDI-TOF-TOF-MS. Mass spectral profiles were interrogated in the m/z region <6 kDa using k-nearest neighbour clustering algorithm. All CNTs were cytotoxic. J774 cells exhibited mass spectral patterns specific to the CNT exposures. Data-mining revealed an elevation in cellular endothelin-1, a pro-inflammatory and mitogenic peptide, and a decrease in cytoplasmic lactate dehydrogenase levels, an indicator of cell membrane permeability, notably in response to the oxidized CNTs. Elevation of o-tyrosine, consistent with formation of reactive oxygen species, was coherent with proteomic changes. The increased potency can be attributed to surface modifications and structural changes in oxidized CNTs, namely increased specific surface area and pore size, and presence of carboxylic groups. Our observations under specific *in vitro* conditions indicate that surface functionalities, and not the metal contaminants, are driving the biological reactivity of these CNTs.

KEYWORDS: carbon nanotubes, surface functionality, toxicity, cytotoxicity, *in vitro*, proteomics, mass spectrometry

ABBREVIATIONS

CNT	carbon nanotube
SWCNT	single-wall carbon nanotube

*Address correspondence and reprint requests to:
Dr. P. Kumarathasan,
Room 233A, Environmental Health Centre,
0803C Tunney's Pasture, Ottawa,
Ontario, K1A 0K9, Canada.
premkumari.kumarathasan@hc-sc.gc.ca
[#]P. Kumarathasan and D. Das are first authors

MWCNT	multi-wall carbon nanotube
PV	pore volume
SSA	specific surface area
HPLC	high-performance liquid chromatography
MTS	3-(4,5-dimethylthiazol-2-yl) -5-(3-carboxymethoxyphenyl) -2-(4-sulfophenyl)-2H-tetrazolium
MALDI	matrix assisted laser desorption ionization
TOF	time of flight
MS	mass spectrometry
PBS	phosphate buffered saline
ROS	reactive oxygen species

INTRODUCTION

In recent years, proteomics approach has gained momentum for biomarker analysis in toxicology, diseases and therapeutics. Identification of protein markers relevant to biological changes can contribute to the understanding of mechanistic pathways and risk associated with contaminant exposures and pathologies. Proteomics-based biomarker discovery has engaged several well characterized and robust technologies in which mass spectrometry plays a central role. Protein separation by 2D-gel electrophoresis followed by mass spectrometry (MS) or tandem mass spectrometry is a classical method used in identification and quantitation of proteins in mixtures [1, 2]. The two most commonly used MS methods are based on matrix assisted laser desorption ionization (MALDI) or electrospray ionization (ESI) in association with mass analysers such as time of flight (TOF), quadrupole (Q), ion trap (IT), linear ion trap (LIT), orbitrap, Fourier transform ion cyclotron resonance, or combinations of these mass analyzers (e.g. TOF-TOF, QTOF).

Shotgun proteomic analyses carried out on clarified proteins or their tryptic digests using matrix-assisted laser desorption ionization time-of-flight mass spectrometry (MALDI-TOF-MS) or by liquid chromatography-mass spectrometry (2D LC-MS) techniques are alternatives to gel-based proteomic procedures. These methods are typically used for high throughput protein expression analyses [3-5]. Zhang *et al.* [6] have applied a clinical proteomic strategy based on direct MALDI-TOF-MS analyses followed by bioinformatic data-mining of spectral differences to investigate changes in plasma peptide and protein fingerprints to compare normal *vs.* disease states. MALDI-TOF-MS analysis is less affected by impurities such as salts and detergents, and the same sample can be used in tryptic peptide scanning for peptide mass fingerprinting (PMF) as well as tandem MS/MS analyses for peptide sequencing and protein marker identification. This technology, unlike LC-ESI-tandem MS/MS analyses, provides high throughput compatibility and sensitivities in atomole range.

Emerging pollutants include classes of nanomaterials that are being produced currently in larger quantities and have found applications as fillers, catalysts, semiconductors, cosmetics, microelectronics, pharmaceuticals, drug carriers, energy storage and anti-friction coatings [7, 8] due to their unique electrical, optical and mechanical properties. Incorporation of engineered nanomaterials into household, personal and industrial products will enhance risk of human and ecosystem exposures during production, transportation, use, and disposal. Carbon nanotube (CNT) is one such nanomaterial which has enormous potential for biomedical and other applications [8]. Carbon nanotubes can be synthesized as single-walled (SW) or multi-walled (MW) forms. Variation in physicochemical properties of CNTs has been reported even between batches using the same synthetic parameters [9]. Moreover, post-synthesis modifications, such as removal of metallic and amorphous impurities or specific surface functionalization, result in variants of CNTs [10].

Although public awareness of nanotechnology is on the rise, very little data are available to establish with reasonable clarity the safety or hazard of these materials [11]. Data published so far in the literature are sometimes inadequate and often not comparable due to lack of information on physicochemical characterization of these materials [12-22]. Thus, there is an urgent need for proper evaluation of toxicological properties of nanomaterials.

In vitro toxicity testing is valuable as a first tier approach to screen toxicity of variants of CNTs to guide the more costly and labour intensive *in vivo* exposure studies on materials of contrasting biological reactivity. *In vitro* studies are amenable to high throughput screening for relative potencies of a large number of materials of varying

physicochemical properties. Our objective in this study was to apply proteomic analyses to identify potential toxicity pathways of pristine single-walled (SWCNT-P), pristine multi-walled (MWCNT-P), oxidized single-walled (SWCNT-O) and oxidized multi-walled (MWCNT-O) CNTs.

EXPERIMENTAL

Material and reagents

Single-walled carbon nanotubes were synthesized by a pulsed laser-oven method using cobalt and nickel as catalysts [23]. Multi-walled carbon nanotubes were purchased from Sun Nanotech (China; >80% purity; 10-30 nm in diameter), and were produced by chemical vapour deposition using iron as catalyst. The murine monocytic cell line J774.1 was purchased from American Type Culture Collection (ATCC, Manassas, USA). Serum-free medium was obtained from Hyclone (Utah, USA). All other cell culture medium and supplements were purchased from BRL (Bethesda, USA).

Oxidation of CNTs

Carbon nanotubes were oxidized by the following procedure. Two hundred mg of either single-walled or multi-walled CNT was dispersed in a 3:1 (v/v) mixture of sulphuric acid (96%) and nitric acid (70%) and sonicated for 2 hours. After sonication, the acidified CNT mixture was diluted with deionized water and filtered using 0.45 μm Whatman filters (Fisher Scientific, Ottawa, Canada). Carbon nanotubes were rinsed with water until the washings showed a pH > 5. The oxidized CNTs were then dispersed in deionized water by sonication for 30 minutes. The precipitate containing impurities such as amorphous carbon was discarded and the top layer containing suspended CNTs was centrifuged at 12,000 x g for 20 minutes. The resulting solid material was collected and dried in an oven at 60ºC overnight. Materials thus collected were oxidized CNTs.

Surface area and pore volume

Surface area and pore volume of CNTs were calculated from nitrogen adsorption and desorption measurements at 77 K using a Coulter Omnisorp 100 gas analyzer. Before exposure to nitrogen, all CNT samples were degassed at 80°C under high vacuum (10^{-5} Torr). Specific surface area (S_{BET}) was determined from the linear part of the BET plot (P/P_0 = 0.05 - 0.15).

Electron microscopy (EM)

Samples of SWCNTs were dispersed in methanol by sonication and dropped onto holey carbon grids. Images of SWCNTs were taken using a Philips CM12 transmission electron microscope (Oregon, USA) operating at 80kV, following the procedure of Kingston *et al.* [23]. Images of MWCNTs were taken using a JOEL JSM-5600 Digital Scanning Electron Microscope (Tokyo, Japan) after coating the sample with gold following the procedure of Salam [24].

Fourier transform infrared (FTIR) analysis

FTIR spectroscopic analyses of CNT variants were performed on an ABB Bomem MB Series FTIR spectrometer (Victoria, Australia) using KBr pellets following the method reported by Das *et al.* [25].

Analysis of metal content

Metal contents of pristine and oxidized CNTs were analyzed using Inductively Coupled Plasma-Atomic Emission Spectroscopy (ICP-AES, Varian Vista-Pro, Mulgrave, Australia) on the acid-digested samples (n = 3 per CNT group). In brief, carbon nanotube samples were digested in 50% HNO_3 for 8 hours at 80°C. These nanotubes were separated by filtration and metal contents in filtrates were analyzed against reagent blank by ICP-AES according to Kim and Jo [26].

Preparation of CNTs for *in vitro* exposures

All four types of carbon nanotube variants were suspended in a small Dounce glass-glass homogenizer at a concentration of 10 mg/mL in phosphate buffered saline (PBS) containing 0.01% Tween-80 [27]. After sonication for 10 minutes in an ultrasonic water bath, these stock CNT suspensions were stored frozen at -40°C until their use in cell culture experiments.

Cell culture and CNT exposure conditions

J774 cells were propagated in Dulbecco Modified Minimum Essential Medium (DMEM) supplemented with foetal bovine serum (10% v/v), L-glutamine (4mM), penicillin (100 IU/mL) and streptomycin

(100 μg/mL). Cells were propagated in 75 cm^2 tissue culture flasks at 37°C in 5% CO_2 and 75% relative humidity. Monolayer of J774 cells were trypsinized and washed with complete cell culture medium. Cell pellets were suspended in fresh medium and the cell density was adjusted to $4x10^5$ cells/mL. The cells were seeded in 96-well cell culture plates at 0.1 mL/well and the plates were incubated at 37°C for 24 hours. Culture medium was replaced with serum-free medium and plates were re-incubated at 37°C for 24 hours. The working CNT suspensions were prepared by dilution of the stock CNT suspensions in serum-free medium followed by sonication. Pristine and oxidized SWCNTs and MWCNT suspensions (0.1 mL/well) were added to the cell culture wells at different doses, ranging from 0-100 $\mu g/cm^2$, and the cell culture plates were incubated again at 37°C for 24 hours. Separate series of plates were prepared for the AlamarBlue assay, the MTS assay, and proteomic analyses.

Cytotoxicity assays

Cytotoxicity was assessed by AlamarBlue and MTS assays. The AlamarBlue assay was performed by adding 50 μL of the diluted reagent (40% v/v with serum-free culture medium) to each well, followed by incubation at 37°C for 4 hours. After centrifugation at 350 x g for 10 minutes, 0.1 mL of culture supernatant was transferred into a fresh 96-well plate. Fluorescence was measured at λ_{Ex} = 530 and λ_{Em} = 590 nm (Cytofluor®, Mississauga, Canada). For the MTS (3-(4,5-dimethylthiazol-2-yl)-5-(3-carboxymethoxyphenyl)-2-(4-sulfophenyl)-2H-tetrazolium) assay, 50 μL of diluted reagent (40% v/v in serum free medium) was added to the wells. Plates were incubated at 37°C for 4 hours, centrifuged at 350 x g for 10 minutes, and 0.1 mL aliquot from each well was transferred into fresh 96 well plates. Absorbance was measured at 490 nm (Spectramax, Molecular Devices, Sunnyvale, USA).

HPLC analysis of o-tyrosine

Cell culture supernatants from the proteomics plates were recovered, centrifuged at 350 x g for 10 minutes, transferred to clean plates, stabilized with preservatives butylated hydroxytoluene and diethylenetriaminepentaacetic acid [28], and frozen until processed for analysis of o-tyrosine. o-Tyrosine was analyzed using a HPLC-Coularray system (ESA, Chelmsford, USA). The HPLC system consists of a solvent delivery module (Model 582), an autosampler (Model 542) and a Coularray detector (Model 5600A). The detector unit consists of eight porous composite carbon electrodes in series and Ag/AgCl reference electrode. The detectors were maintained at positive potentials of 0, 150, 300, 450, 600, 650, 700, and 800 mV. Twenty μL of the clarified cell supernatant sample was injected onto a Zorbax C18 reverse phase column [28]. The target analytes were eluted isocratically using citrate-acetate mobile phase at a flow rate of 1 mL/min and analyzed as described by Kumarathasan *et al.* [28]. Blank samples were run among sample runs to verify any cross contamination.

Sample processing for MALDI-TOF-TOF-MS analysis

The cell monolayers from the proteomics plates were rinsed gently twice with PBS. Lysis solution (20 μL) consisting of antiprotease cocktail (Fisher Scientific, Ottawa, Canada) diluted in deionized water, was added to each well. The cells were lysed by three complete cycles of freezing at -40°C for 1 hour and thawing at room temperature for ½ hour. The cell lysates were transferred into 250 μL eppendorf tubes and kept at -80°C until used. Thawed cell lysates were vortexed (5 seconds), sonicated (5 seconds) and vortexed (5 seconds) again. The lysates were centrifuged at 10,000 x g for 15 minutes to separate the CNTs and other cell debris from the lysates. Molecular weight cut-off (MWCO) filters (50 kDa) were pre-wetted by passing 300 μL deionized water at 10,000 x g for 15 minutes (filtrate discarded). One 10 μL aliquot of each cell lysate was diluted with 170 μL of deionized water, filtered through the 50 kDa MWCO filter by centrifugation at 10,000 x g for 30 minutes, and the filtrate was collected (<50 kDa fraction). The residue collected on the filter (>50 kDa fraction) was treated with 180 μL of 10% acetonitrile containing 0.1% TFA in water and vortexed gently (2 seconds). The MWCO filters were inverted and centrifuged at 10,000 x g for 15 minutes. This recovered >50 kDa fraction was subjected to tryptic digestion at 37°C

overnight as described before [2]. The tryptic digest was filtered through 50 kDa MWCO filters by centrifugation at 10,000 x g for 30 minutes, and the filtrate containing the peptides for MS analysis was collected. All filtrates were evaporated and stored at -80°C until analysis by MALDI-TOF-TOF-MS.

MALDI -TOF-TOF-MS analysis

One μL of the above processed samples (n = 9 per exposure dose) was spotted in duplicates at the centre of the sample location on a 384/600 anchor chip target plate (Bruker Daltonics). One μL of matrix solution (1 mg/mL α-cyano-4-hydroxy cinnamic acid in 50% acetonitrile, 0.1% TFA) was added on top of the sample spot and was mixed as described previously [2]. An on-target washing of the sample spot was carried out by placing 2.5 μL of cold 1% TFA in water on the dried sample spot, and the liquid was removed after 10 seconds. Washed spots were dried and analyzed by MALDI-TOF-TOF-MS. Analyses were carried out using a Bruker Daltonics Autoflex III time-of-flight mass spectrometer (Bruker Daltonics, Bremen, Germany) equipped with a Smart Beam™ laser emitting at 355 nm wavelength, a 1 GHz sampling rate digitizer, a pulsed ion extraction source, and a TOF-TOF-MS analyzer. Calibration was done using external protein and peptide calibration standards (Bruker Daltonics). Detection was carried out in a linear or reflectron positive mode. In a typical experiment, a composite spectrum (total of 4000 shots) was obtained by summation of twenty 200-shots of individual spectra. The sampling sites were selected randomly for every sample in order to obtain homogenous sampling. The data acquisition and processing were carried out using the Flex Control 3.3 and Flex analysis 3.3 software, respectively. Mass spectra were data mined using k-nearest neighbour algorithm (ClinPro Tools version 2.0, Bruker) to identify candidate biomarkers. These candidate biomarkers were further characterized by MS/MS analyses in *Lift* mode by selection and fragmentation of parent ions. The MS/MS data obtained were queried against proteomic databases (SwissProt, MSDB, NCBInr) using BioTools software and MASCOT search engine for protein identification.

Statistical analysis

Cytotoxicity was measured on cells exposed to doses 0, 3, 10, 30, 100 μg/cm^2. Proteomic analyses were conducted on cells exposed to doses 0, 30, 100 μg/cm^2. o-Tyrosine assays were conducted on supernatants of naïve control cell and cells exposed to the high dose 100 μg/cm^2. Statistical analyses were carried out using SigmaStat v3.5 software (SPSS Inc, Chicago, IL). Differences between the treatment groups were determined by three-way ANOVA with factors carbon nanotube CNT (SWCNT, MWCNT), modification MOD (P pristine, O oxidized), and DOSE, two-way ANOVA with the type of carbon nanotube CNTMOD (SWCNT-P, SWCNT-O, MWCNT-P, MWCNT-O) and DOSE as factors, or one-way ANOVA with CNTMOD as factor (Control, SWCNT-P, SWCNT-O, MWCNT-P, MWCNT-O) as appropriate. Tukey's pair wise multiple comparison procedure was applied. Statistical significance was considered at $p < 0.05$.

RESULTS AND DISCUSSION

Transmission electron microscopy (TEM) analyses of pristine SWCNTs and MWCNTs revealed that these materials were highly entangled tubes with diameters of *ca* 5 and *ca* 20 nm, respectively. Although it was difficult to measure the length of the CNTs from TEM images, length of some CNT tubes were measured to be at least 1 μm for SWCNTs and ≥ 500 nm for MWCNTs. Both the pristine SWCNT and MWCNT contained amorphous carbonaceous impurities along with the nanotube structures. TEM analysis also revealed that the oxidation process altered some physicochemical characteristics of CNTs (Figure 1). For instance, shortened nanotube length of oxidized CNTs was probably due to some carbon vacancy defects and some morphological changes on the surface of the nanotubes (data not shown). Similar changes have been previously reported with oxidation of CNTs [29].

Pristine MWCNTs exhibited higher specific surface area (SSA) and pore volume (PV) compared to pristine SWCNTs (SSA, SWCNT-P, 89 m^2/g, MWCNT-P, 106 m^2/g; PV, SWCNT- P, 0.30 cc/g, MWCNT-P, 0.43 cc/g). Meanwhile, SSA and PV values were lower for both the oxidized CNTs compared to their pristine counterparts

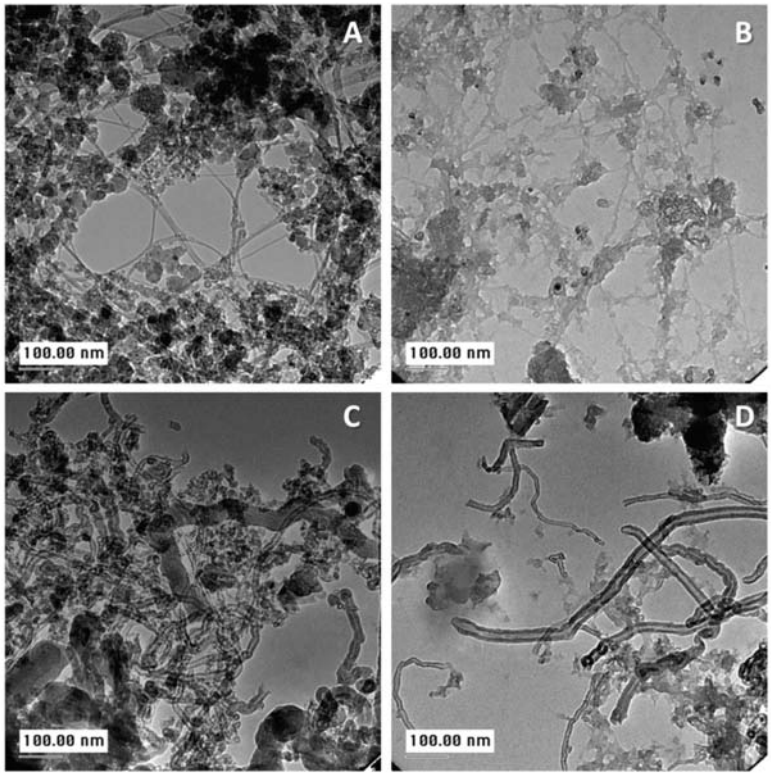

Figure 1. Transmission electron microscopy image of pristine and oxidized carbon nanotubes. A, SWCNT pristine. B, SWCNT oxidized. C, MWCNT pristine. D, MWCNT oxidized.

(SSA, SWCNT-O, 21 m^2/g, MWCNT-O, 23 m^2/g; PV, SWCNT-O, 0.11 cc/g, MWCNT-P, 0.12 cc/g). Surface area reduction due to CNT oxidation has been reported before [29].

Metal content analyses by ICP-MS indicated that the oxidation process markedly reduced the % content of Co (SWCNT-P vs SWCNT-O, 1.24 ± 0.13 vs 0.21 ± 0.02) and Ni (1.16 ± 0.13 vs 0.19 ± 0.03), used as catalysts in the production of pristine SWCNTs, as well as the co-contaminants Fe (0.32 ± 0.4 vs 0.1 ± 0.01) and Mo (0.28 ± 0.02 vs 0.04 ± 0.01). The oxidation of MWCNTs also resulted in slight decrease of Fe (MWCNT-P vs MWCNT-O, (1.08 ± 0.03 vs 0.52 ± 0.12) and Ni (0.62 ± 0.04 vs 0.44 ± 0.1). These results indicate that the acid treatment employed in the oxidation process reduced the levels of metal contaminants in the CNT structures.

Analysis of CNT variants by FTIR identified the surface functionalities formed as a result of the oxidative process. The spectrum of oxidized MWCNTs and SWCNTs exhibited IR vibrational modes due to C=O stretching at 1730 cm^{-1} and C-O stretching at 1130 cm^{-1}. These bands were not present in their pristine counterparts. This confirms the formation of carboxylic acid (-COOH) groups on the CNT surface due to the oxidative process [30]. Our dispersion experiments revealed that both the oxidized CNTs were more dispersed in serum-free cell culture medium containing 0.01% Tween-80 than the pristine CNTs. This could be due to the presence of surface carboxylic groups in the oxidized CNTs that lead to increased hydrophilicity of these materials. It is interesting to note here that, although in the dry state the oxidized CNTs exhibited lower surface area compared to pristine counterparts, in the cell culture medium the increased dispersion of oxidized CNTs and thus increased surface area of reaction, as opposed to their pristine counterparts, reinforces the notion of the presence of polar surface groups in oxidized CNTs.

In the analyses of biological responses, differences between the treatment groups were first verified in three-way ANOVAs with factors carbon nanotube

CNT (SWCNT, MWCNT), modification MOD (P pristine, O oxidized), and DOSE (0, 3, 10, 30, 100 μg/cm^2). The AlamarBlue assay showed a three-way factor interaction (CNT x MOD x DOSE, $p < 0.001$) and main effects for all factors CNT, MOD and DOSE ($p < 0.001$). The MTS assay in three-way ANOVA showed main effects for factors MOD ($p = 0.021$) and DOSE ($p = 0.001$). Therefore, these preliminary statistical analyses confirmed that cellular responses were determined by all three factors, namely the type of CNTs (single-wall vs multi-wall), the oxidation process (pristine vs oxidized), and the dose of material. All data were then analysed by two-way ANOVA with the type of carbon nanotube CNTMOD (SWCNT-P, SWCNT-O, MWCNT-P, MWCNT-O) and DOSE as factors.

J774 is a murine monocyte-derived macrophage cell line from BALB/c mice. The cells process particles by phagocytosis [31]. All CNTs caused dose-dependent decrease of AlamarBlue reduction (two-way ANOVA, CNTMOD x DOSE interaction, $p < 0.001$) and MTS reduction (two-way ANOVA, CNTMOD main effect, $p = 0.041$; DOSE main effect, $p < 0.001$), with significant ($p < 0.05$) changes at the 30 and 100 μg/cm^2 doses (Figure 2). Decreased reduction of the AlamarBlue and MTS reagents reflects an impact of treatments on the redox state of the cells and decreased ability to reduce co-factors in metabolism. The factor MOD (pristine vs oxidized) was also statistically significant by multi-way ANOVA (AlamarBlue, $p < 0.001$; MTS, $p = 0.021$), indicating that overall toxic potency of the CNTs was enhanced by the

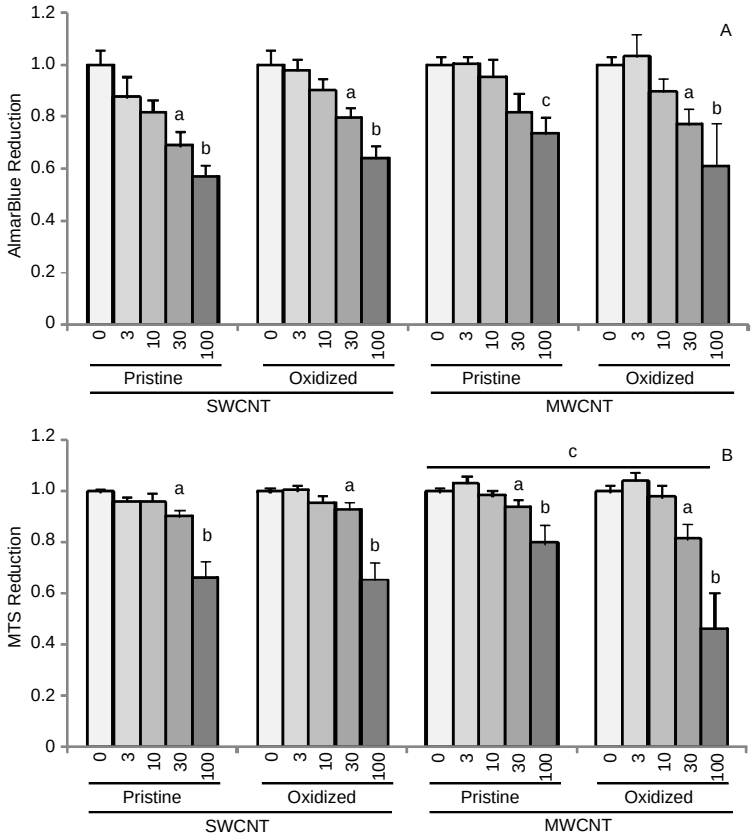

Figure 2. Reduction of AlamarBlue (A) and MTS (B) after exposure to variants of carbon nanotubes. All data are normalized relative to control (0 μg/cm^2) and are presented as mean ± SEM (n = 9 replicates). A. Two-way ANOVA, CNTMOD x DOSE interaction, $p < 0.001$. Tukey's comparison procedure for DOSE within CNTMOD. a, 0 vs 30, $p < 0.05$. b, 30 vs 100, $p < 0.05$. c, 0 vs 100, $p < 0.05$. B. Two-way ANOVA, CNTMOD main effect, $p = 0.041$, and DOSE main effect, $p < 0.001$. Tukey for DOSE within CNTMOD. a, 0 vs 30, $p < 0.05$. b, 30 vs 100, $p < 0.05$. Tukey for CNTMOD main effect. c, MWCNT-O vs MWCNT-P, $p < 0.05$.

oxidation process to remove metals. Cytotoxic potency ranking (from group means) of the CNTs in the AlamarBlue assay was MWCNT-O > MWCNT-P > SWCNT-O > SWCNT-P. Potency ranking in the MTS assay was MWCNT-O ≥ SWCNT-O > SWCNT-P ≥ MWCNT-P.

o-Tyrosine produced from hydroxylation of phenylalanine moiety in protein can serve as a marker of cellular oxidative stress. Engineered nanomaterials have been shown to perturb the oxidative balance of cells, resulting in intracellular and extracellular free radical generation [11, 21, 32-36]. These reactive oxygen and nitrogen species can cause damage to various cellular macromolecules (protein, lipid or nucleic acid), resulting in abnormal cellular function. o-Tyrosine was significantly elevated in the cell culture supernatants associated with exposure to the oxidized CNTs compared to naïve control cells (one-way ANOVA, p = 0.003) (Figure 3). Potency ranking in the o-tyrosine assay was SWCNT-O ≥ MWCNT-O > MWCNT-P ≥ SWCNT-P. Although previous reports have associated CNT toxicity with ROS formation due to presence of metals [21], we show here that even though metal contents are comparably lower in the oxidized CNTs, as opposed to their pristine counterparts, o-tyrosine formation is increased in cells exposed to oxidized CNTs. This implies that pathways other than metal redox-cycling can be involved in ROS production as well. The enhanced biological reactivity of the CNTs after oxidation can probably be attributed to the presence of surface polar groups such as carboxylic acid moieties.

Analyses of J774 cellular proteomic profiles provide additional information in terms of understanding toxicity pathways. Initial direct analysis of cellular proteomic changes in cell lysates revealed experimental artefacts due to contaminating CNTs that were not completely eliminated by centrifugation at 12,000 x g for 30 minutes. Clarification of J774 cell lysates using 50 kDa molecular weight cut-off filtration removed the interference by CNTs (Figure 4). Mass spectral data generated by the optimized sample preparation method was mined using k-nearest neighbor algorithm to identify candidate protein markers of CNT exposures. These markers

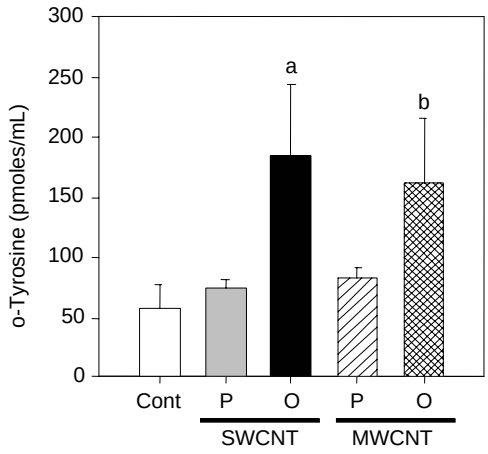

Figure 3. Analysis of the reactive oxygen species marker o-tyrosine in the cell culture supernatants of control (Cont) J774 cells and after 24h incubation with 100 ug/cm^2 SWCNT-P, SWCNT-O, MWCNT-P and MWCNT-O. Mean ± SEM for n = 4 replicates. One-way ANOVA on rank, p = 0.006. Tukey's multiple-comparison procedure. a, SWCNT-O vs Cont, p = 0.014, and SWCNT-O vs SWCNT-P, p = 0.032. b, MWCNT-O vs Cont, p = 0.028.

were further investigated by MS/MS analysis followed by MASCOT database search for protein identification (Table 1). Relative quantitation of the markers revealed changes in the profiles of endothelin-1 (CNTMOD main effect, p = 0.025, and DOSE main effect, p < 0.001; Figure 5A) and lactate dehydrogenase (CNTMOD main effect, p = 0.038, and DOSE main effect, p = 0.039; Figure 5B) in cell lysates. Endothelin-1 (ET-1) is a pro-inflammatory and mitogenic peptide, produced by macrophages and endothelial cells, and which has been associated with adverse pulmonary and cardiovascular effects of inhaled fine particles [37]. Increased cellular levels of ET-1 imply transcriptional activation of the pre-pro ET-1 gene and de novo synthesis of the peptide. Potency ranking for ET-1 was SWCNT-O > MWCNT-O > MWCNT-P > SWCNT-P. Decrease of the cellular content of the cytoplasmic enzyme lactate dehydrogenase (LDH) is consistent with cell membrane permeability during phagocytosis and cell injury with release of the intracellular LDH. Potency ranking for decreased cell LDH content (increased release) was MWCNT-O > SWCNT-O ≥ MWCNT-P > SWCNT-P. The pattern of responses of both markers correlated with the

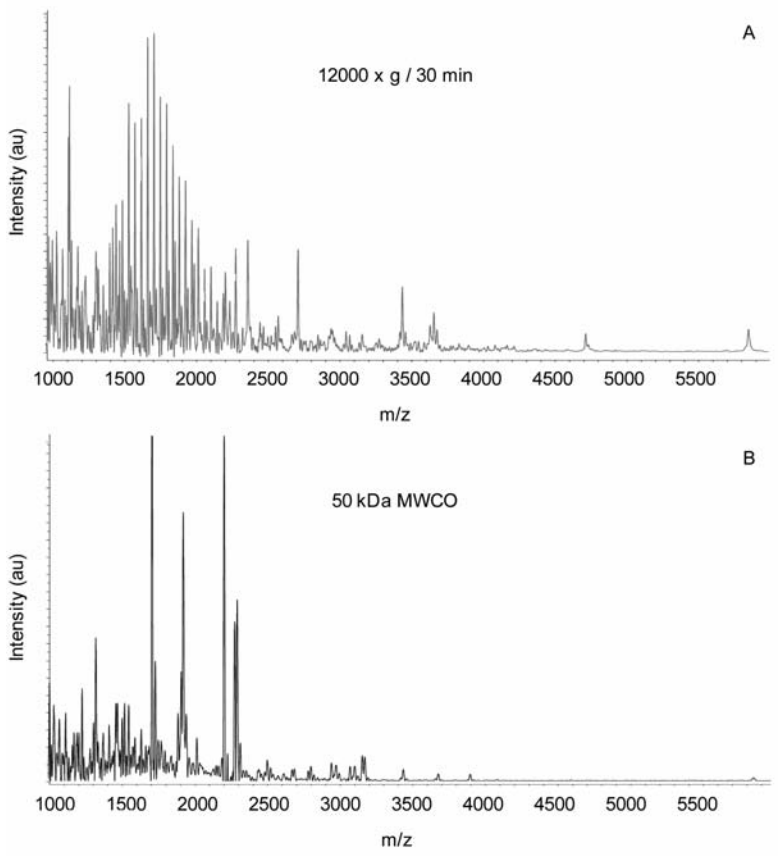

Figure 4. Relieving experimental artefacts in MALDI-TOF-MS analysis of cell lysates obtained after J774 cells were exposed to CNTs. A. Clarification of cell lysates by centrifugation 12000 x g for 30 minutes prior to trypsin digestion results in experimental artefacts and masking of the peptide profiles. B. Cleanup of cell lysates and tryptic digests on a 50 kDa MW cut-off filter removes interference by CNTs.

Table 1. Candidate Protein Markers from MS Data-Mining.

PROTEIN / PEPTIDE	FUNCTION / MARKER	Pearson Product Moment Correlation	
		AlamarBlue	MTS
Endothelin-1 ↑	Inflammatory and mitogenic peptide	p = 0.014	p = 0.034
Lactate dehydrogenase ↓	Metabolic process / membrane permeability	p = 0.027	p = 0.057
Immunoglobulin kappa chain ↑	Antigen binding and effector function		
Immunoglobulin heavy chain ↑	Antigen binding and effector function		
T-cell receptor β-chain ↑	Antigen presentation		
MHC II bound peptide fragment ↑	Antigen presentation		
α-Endosulfine ↑	Protein phosphatase inhibitor, interferes with mitosis		
β-Actin ↓	Cytoskeletal rearrangement		
Tropomodulin ↓	Cytoskeletal rearrangement		
T-cell receptor α V region ↓	Antigen presentation		
T-cell receptor delta chain ↓	Antigen presentation	p = 0.007	p = 0.009
Homeobox protein 4.2 ↓	Transcription factor, cell survival, proliferation		p = 0.014

Note: Up regulation (↑) and down regulation (↓).

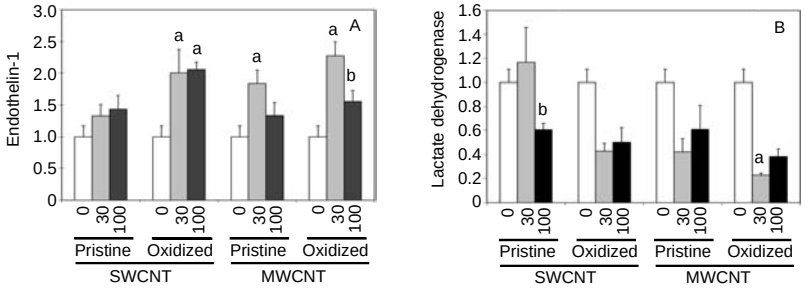

Figure 5. Mass spectral peak area profiles of endothelin-1 (A) and lactate dehydrogenase (B) in cell lysates. A. Two-way ANOVA, CNTMOD main effect, p = 0.025, and DOSE main effect, p < 0.001. Tukey for DOSE within CNTMOD. a, 0 vs 30, 0 vs 100, p < 0.05. b, 30 vs 100, p < 0.05. B. Two-way ANOVA, CNTMOD main effect, p = 0.038, and DOSE main effect, p = 0.039. Tukey for DOSE within CNTMOD. a, 0 vs 30, 0 vs 100, p < 0.05. b, 30 vs 100, p < 0.05.

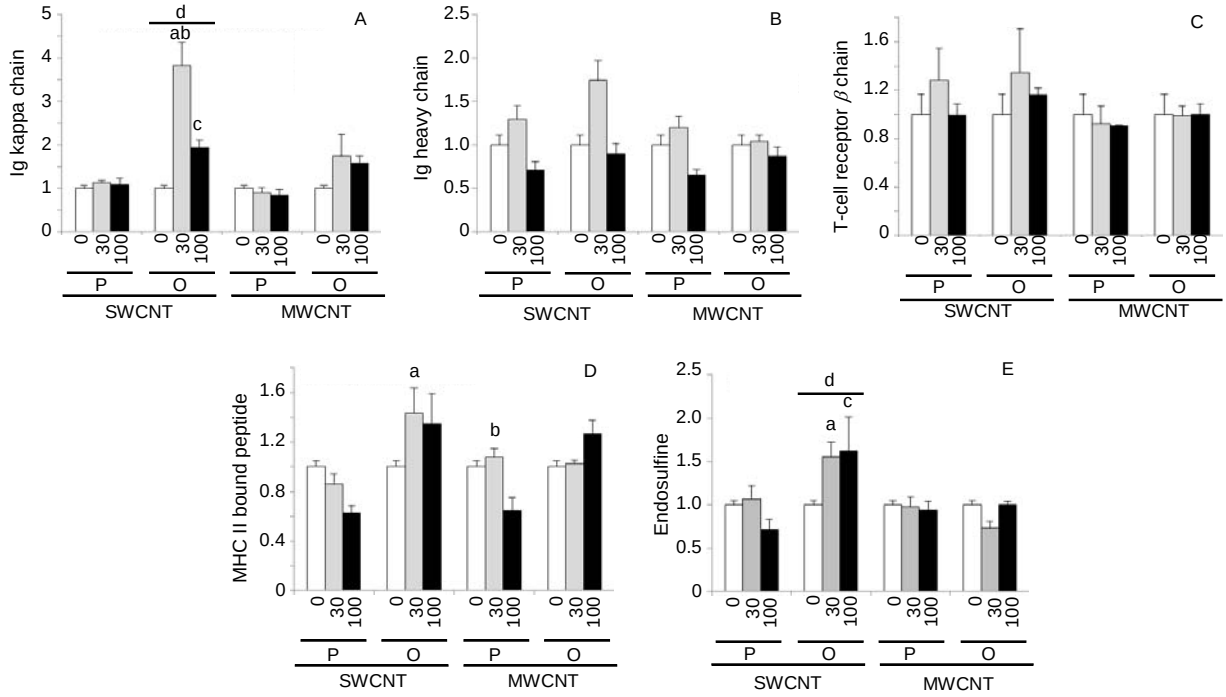

Figure 6. Mass spectral peak area profiles for immunoglobulin kappa chain (A) and heavy chain (B), T-cell receptor β chain (C), MHC II bound peptide fragment (D) and endosulfine (E) in cell lysates. Two-way ANOVA, CNTMOD x DOSE interactions, p < 0.05. Tukey for DOSE within CNTMOD. a, 0 vs 30, p < 0.05. b, 30 vs 100, p < 0.05. c, 0 vs 100, p < 0.05. Tukey for CNTMOD main effect. d, SWCNT-O > others.

two cytotoxicity markers AlamarBlue and MTS (Pearson Product Moment Correlation, Table 1), consistent with increased potency of oxidized CNTs over pristine CNTs.

Several of the markers identified by k-nearest neighbor analysis are involved in antigen processing and presentation, cytoskeletal rearrangement, and cell proliferation typical of the functions of macrophages. Backward stepwise regression analysis indicated that cell viability as assessed by AlamarBlue can be predicted (p < 0.05) by a linear combination of LDH, tropomodulin and homeobox protein HOX 4.2. Similarly, potency in the MTS assay can be predicted (p < 0.05) by linear

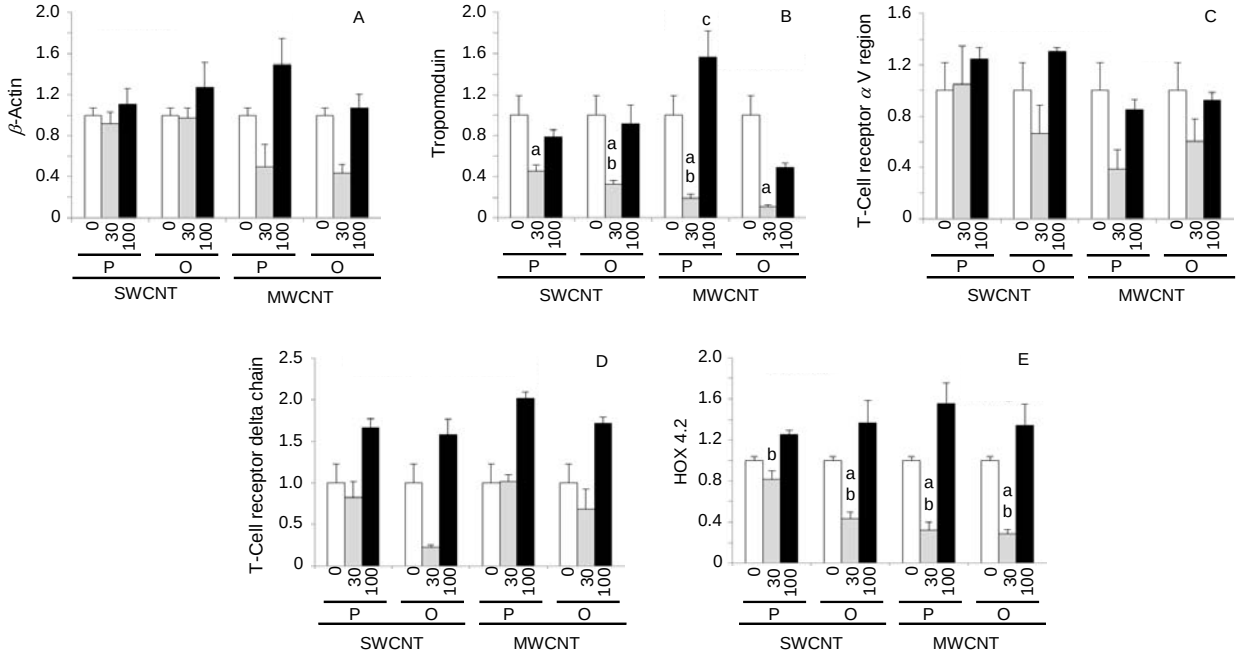

Figure 7. Mass spectral peak area profiles for β-actin (A), tropomodulin (B), T-cell receptor α V region (C), T-cell receptor delta chain (D) and HOX 4.2 (E) in cell lysates. Two-way ANOVA, CNTMOD x DOSE interactions, $p < 0.05$. Tukey for DOSE within CNTMOD. a, 0 vs 30, $p < 0.05$. b, 30 vs 100, $p < 0.05$. c, 0 vs 100, $p < 0.05$.

combination of LDH, tropomodulin, HOX 4.2 and T-cell receptor alpha V region. Two distinct patterns of responses to CNT exposures were observed among the profiles of candidate proteomic markers, as reflected in increase (Figure 6) or decrease (Figure 7) of the markers in response to CNT exposure, notably at the 30 μg/cm^2 dose.

Understanding the toxicity of ultrafine and nanoparticles, which are in fact complex chemical and physical matrices, is challenging [38, 39]. Conducting proteomic analyses along with the classical cellular cytotoxicity assays can shed light into the *in vitro* toxicity mechanisms underlying CNT exposures.

CONCLUSIONS

Physicochemical characteristics of CNT variants, namely surface area, chemical composition and surface polarity, clearly impacted biological changes in J774 cells after *in vitro* exposure. Our results indicated that CNT exposure-related ROS formation can also form by pathways other than metal-catalyzed reactions. Proteomic analysis of J774 cell contents revealed that mechanistic pathways relevant to important cellular functions were differentially affected by CNT variants, in relation to their physicochemical properties. These results suggest that protein profiling is a promising tool in determining CNT-specific changes in biological responses and unraveling toxicity pathways in combination with cellular cytotoxicity data.

ACKNOWLEDGEMENTS

The authors are grateful to Mr. Yunus Siddiqui for the cell culture work. This work was supported by Health Canada (CMP Nano Initiative-810478 and EHSRB-4320105).

REFERENCES

1. Issaq, H. and Veenstra, T. 2008, Biotechniques, 44, 697.
2. Kumarathasan, P., Mohottalage, S., Goegan, P., and Vincent, R. 2005, Anal. Biochem., 346, 85.

3. Mohottalage, S., Karthikeyan, S., Vincent, R., and Kumarathasan, P. 2007, Can. J. Anal. Sci. Spectrosc., 52, 243.
4. Mohottalage, S., Vincent, R., and Kumarathasan, P. 2009, JAOAC Inter., 92, 1652.
5. Motoyama, A. and Yates, J. R. III. 2008, Anal. Chem., 80, 7187.
6. Zhang, X., Leung, S. M., Morris, C. R., and Shigenaga, M. K. 2004, J. Biomol. Techlol., 15, 167.
7. Donaldson, K., Stone, V., Tran, C. L., Kreyling, W., and Borm, P. J. 2004, Nanotoxicol. Occup. Environ. Med., 61, 727.
8. Farre, M., Gajda-Schrantz, K., Kantiani, L., and Barcelo, D. 2009, Anal. Bioanal. Chem., 393, 81.
9. Cui, H., Zhou, O., and Stoner, B. R. 2000, J. Appl. Phys., 88, 6072.
10. Nowack, B. and Bucheli, T. D. 2007, Environ. Pollut., 150, 5.
11. Stern, S. T. and McNeil, S. E. 2008, Toxicol. Sci., 101, 4.
12. Herzog, E., Byrne, H. J., Davoren, M., Casey, A., Duschl, A., and Oostingh, G. J. 2009, Toxicol. Appl. Pharmacol., 236, 276.
13. Hirano, S., Kanno, S., and Furuyama, A. 2008, Toxicol. Appl. Pharmacol., 232, 244.
14. Jacobsen, N. R., Pojana, G., White, P., Moller, P., Cohn, C. A., Korsholm, K. S., Vogel, U., Marcomini, A., Loft, S., and Wallin, H. 2008, Environ. Mol. Mutagen., 49, 476.
15. Kagan, V. E., Tyurina, Y. Y., Tyurin, V. A., Konduru, N. V., Potapovich, A. I., Osipov, A. N., Kisin, E. R., Schwegler-Berry, D., Mercer, R., Castranova, V., and Shvedova, A. A. 2006, Toxicol. Lett., 165, 88.
16. Monteiro-Riviere, N. A., Nemanich, R. J., Inman, A. O., Wang, Y. Y., and Riviere, J. E. 2005, Toxicol. Lett., 155, 377.
17. Sarkar, S., Sharma, C., Yog, R., Periakaruppan, A., Jejelowo, O., Thomas, R., Barrera, E. V., Rice-Ficht, A. C., Wilson, B. L., and Ramesh, G. T. 2007, J. Nanosci. Nanotechnol., 7, 584.
18. Yang, H., Liu, C., Yang, D., Zhang, H., and Xi, Z. 2009, J. Appl. Toxicol., 29, 69.
19. De Nicola, M., Gattia, D. M., Bellucci, S., DeBellis, G., Miccuilla, F., Pastore, R., Tiberia, A., Cerella, C., DeAlessio, M., Antisari, M. V., Marazzi, R., Traversa, E., Magrini, A., Bergamaschi, A., and Ghibelli, L. 2007, J. Phys. Cond. Matter., 19, 395013.
20. Flahaut, E., Durrieu, M. C., Remy-Zolghadri, M., Bareille, R., and Baquey, C. 2006, Carbon, 44, 1093.
21. Pulskamp, K., Diabate, S., and Krug, H. F. 2007, Toxicol. Lett., 168, 58.
22. Yang, S. T., Wang, X., Jia, G., Gu, Y., Wang, T., Nie, H., Ge, C., Wang, H., and Liu, Y. 2008, Toxicol. Lett., 181, 182.
23. Kingston, C. T., Jakubek, Z. J., Denommee, S., and Simard, B. 2004, Carbon, 42, 1657.
24. Salam, M. A. 2006, Chemical modification of multi-walled carbon nanotubes and their potential applications as adsorbents for solid phase extraction from aqueous solutions. PhD Thesis, Carleton University, Ottawa, ON, Canada.
25. Das, D. D., Harlick, P. J. E., and Sayari, A. 2007, Catal. Comm., 8, 829.
26. Kim, M. K. and Jo, W. K. 2006, Inter. Arch. Occup. Environ. Health, 80, 40.
27. Vincent, R., Goegan, P., Johnson, G., Brook, J. R., Kumarathasan, P., Bouthillier, L., and Burnett, R. T. 1997, Fundam. Appl. Toxicol., 39, 18.
28. Kumarathasan, P. and Vincent, R. 2003, J. Chromatogr. A, 987, 349.
29. Kuznetsova, A., Yates, J. T. Jr., Simonyan, V. V., Johnson, J. K., Huffman, C. B., and Smalley, R. E. 2001, J. Chem. Phys., 115, 245.
30. Kathi, J. and Rhee, K. 2008, J. Mat. Sci., 43, 33.
31. Becker, T., Volchuk, A., and Rothman, J. E. 2005, Proc. Nat. Acad. Sci., 102, 4022.
32. Ema, M., Kobayashi, N., Naya, M., Hanai, S., and Nakanishi, J. 2010, Reprod. Toxicol., 30, 343.
33. Kang, S. J., Kim, B. M., Lee, Y. J., and Chung, H. W. 2008, Environ. Mol. Mutagen., 49, 399.
34. Lee, K. J., Nallathamby, P. D., Browning, L. M., Osgood, C. J., and Xu, X. H. 2007, ACS Nano, 1, 133.

35. Marquis, B. J., Love, S. A., Braun, K. L., and Haynes, C. L. 2009, Analyst, 134, 425-439.
36. Murray, A. R., Kisin, E., Leonard, S. S., Young, S. H., Kommineni, C., Kagan, V. E., Castranova, V., and Shvedova, A. A. 2009, Toxicol., 257, 161.
37. Vincent, R., Kumarathasan, P., Goegan, P., Bjarnason, S. G., Guénette, J., Bérubé, D., Adamson, I. Y., Desjardins, S., Burnett, R. T., Miller, F. J., and Battistini, B. 2001, Res. Reports Health Effects Inst., 104, 5.
38. Donaldson, K., Stone, V., Clouter, A., Renwick, L., and MacNee, W. 2001, Occup. Environ. Med., 58, 211.
39. Shvedova, A. A., Kisin, E. R., Porter, D., Schulte, P., Kagan, V. E., Fadeel, B., and Castranova, V. 2009, Pharmacol. Theor., 121, 192.